Biophysical Letter

Lipid Headgroups Modulate Membrane Insertion of pHLIP Peptide

Alexander Kyrychenko,[1] Victor Vasquez-Montes,[1] Martin B. Ulmschneider,[2] and Alexey S. Ladokhin[1,*]
[1]Department of Biochemistry and Molecular Biology, The University of Kansas Medical Center, Kansas City, Kansas; and [2]Department of Materials Science and Engineering, Johns Hopkins University, Baltimore, Maryland

ABSTRACT The pH low insertion peptide (pHLIP) is an important tool for drug delivery and visualization of acidic tissues produced by various maladies, including cancer, inflammation, and ischemia. Numerous studies indicate that pHLIP exists in three states: unfolded and soluble in water at neutral pH (State I), unfolded and bound to the surface of a phosphatidylcholine membrane at neutral pH (State II), and inserted across the membrane as an α-helix at low pH (State III). Here we report how changes in lipid composition modulate this insertion scheme. First, the presence of either anionic lipids, cholesterol, or phosphoethanolamine eliminates membrane binding at neutral pH (State II). Second, the apparent pK_a for the insertion transition (State I $\rightarrow$ State III) is increased with increasing content of anionic lipids, suggesting that electrostatic interactions in the interfacial region modulate protonation of acidic residues of pHLIP responsible for transbilayer insertion. These findings indicate a possibility for triggering protonation-coupled conformational switching in proteins at membrane interfaces through changes in lipid composition.

Received for publication 18 August 2014 and in final form 5 January 2015.

*Correspondence: aladokhin@kumc.edu

Alexander Kyrychenko's present address is V. N. Karazin Kharkiv National University, Kharkiv, Ukraine.

Numerous studies by Engelman, Reshetnyak, Andreev and co-workers demonstrate that a peptide, corresponding to C helix of bacteriorhodopsin, called the pH low insertion peptide (pHLIP), is capable of targeting acidic tissues and inserting into cell membranes (Andreev et al. (1) and references therein). This makes it an important tool for targeting many diseased tissues that create acidic environment (e.g., cancer, inflammation, and ischemia). Dye-labeled pHLIP is able to image mouse tumors in vivo with high specificity (2), demonstrating its potential utility in cancer diagnosis. pHLIP is also capable of selective delivery of cargo molecules (3,4). These properties, combined with low toxicity, demonstrate its high therapeutic potential.

The remarkable properties of pHLIP are a manifestation of its peculiar sequence, which consists of stretches of highly hydrophobic residues interrupted by six titratable acidic residues:

GGEQNPIYWARYADWLFTTPLLLLD-
LALLVDADEGT.

According to the Wimley-White hydrophobicity scales (5), protonation of the glutamates and aspartates of pHLIP results in a total gain of ~20 kcal/mol (3.2 and 3.5 for each residue D and E, respectively) in favorable free energy of partitioning from water into octanol. The gain for interfacial partitioning into the lipid bilayer is smaller, yet significant ~9 kcal/mol (1.3 and 2.0 for protonation of each residue D and E, respectively). All these estimates indicate that membrane interactions of pHLIP will be strongly pH-dependent. Previous studies had firmly established that in phosphatidylcholine bilayers, pHLIP exists in three states as a monomer (6): unfolded and soluble in water at neutral pH (State I), unfolded and bound to the surface of a phosphatidylcholine membrane at neutral pH (State II), and inserted across the membrane as an α-helix at low pH (State III). While the role of sequence variation in pH-triggered insertion of the pHLIP family of peptides has been thoroughly studied (7,8), much less attention has been paid to the effects of lipid composition. Here we investigate the role of lipid headgroups in modulating pHLIP insertion into large unilamellar vesicles (LUVs).

We use tryptophan fluorescence and circular dichroism (CD) to reproduce the hallmarks of the three-state insertion (Fig. 1). Indeed, upon addition of POPC LUV (*top panels*) we observe classical three-state behavior (6), with addition of vesicles at pH 8 causing a blue shift of fluorescence and a marginal increase in helical content (State II, *red lines*), and lowering pH to 4 causing a further spectral shift and formation of an α-helix (State III, *blue line*). The fact that State II is not just a mixture of the other two states has been firmly established in the literature and is also evident from pH titration in Fig. 2 *A*. Much to our surprise, we did not see the same pattern with any other lipid compositions we explored, none of which gave any evidence of the

Editor: Joseph Falke.

http://dx.doi.org/10.1016/j.bpj.2015.01.002

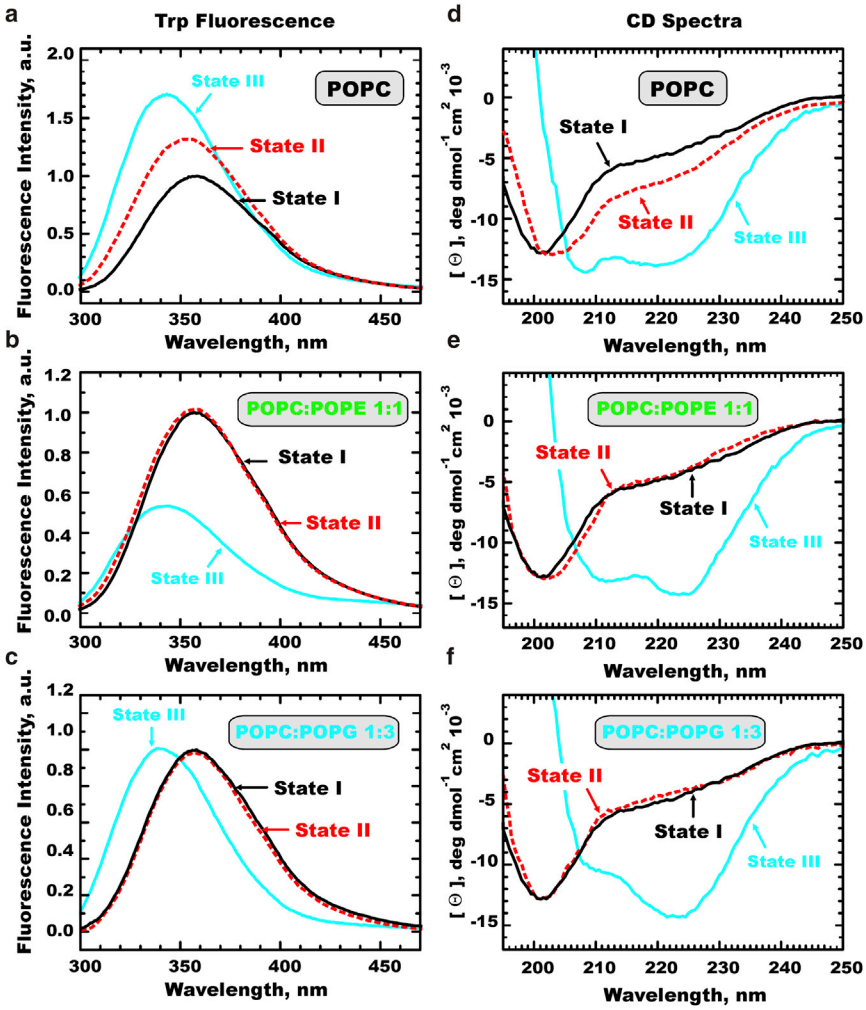

FIGURE 1 Tryptophan fluorescence (*left panels*) and CD spectra (*right panels*) of pHLIP in membranes with different lipid compositions. States I, II, and III correspond to peptide in solution at pH 8, and in the presence of membranes at pH 8 and 4, respectively. To see this figure in color, go online.

presence of the unfolded membrane-bound state at neutral pH. As can be seen in examples presented in Fig. 1, addition of either POPE or POPG eliminates any distinct spectroscopic signature of State II in either CD or fluorescence (i.e., the *black* and *red lines* coincide). On the other hand, acidification led to the expected fluorescence blue shift and folding into a helical conformation, all indicative of efficient formation of State III (*blue lines*).

In the case of anionic lipids, the absence of the interfacially bound state at neutral pH can easily be explained by electrostatic repulsion. State II for cholesterol-, LysoPC-, and POPE-containing membranes suggests that other factors, such as bilayer packing, can influence interfacial partitioning of pHLIP.

To examine the effect of lipid composition on titration of acidic residues in pHLIP, which allows membrane insertion at low pH, we measured pH-dependent spectral shift of tryptophan fluorescence in various vesicles (Fig. 2). We found that increasing fractions of various lipid additions into POPC matrix shifts pK_a values toward less acidic pH (Fig. 2 and Table S1 in the Supporting Material). E.g., changing the POPE fraction from 10 to 50% shifts the pK_a by as much as 0.5 units. Remarkably, the pK_a for pure POPC (i.e., 0% non-PC lipid) does not follow the trend for any of the tested lipid mixtures, suggesting that the transition from State II to III (POPC) and that from State I to III

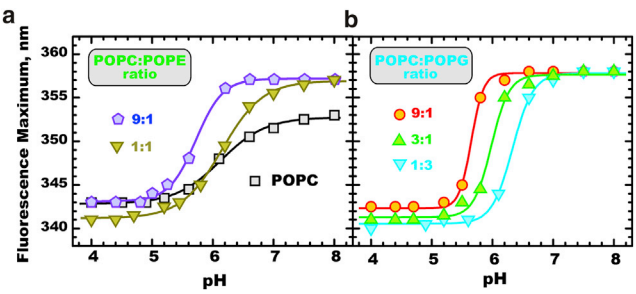

FIGURE 2 Fluorescence spectral maximum changes upon pH titration of 2 μM pHLIP in the presence of LUVs of various compositions (1 mM total lipid). The experimental data were fitted to Eq. S1 in the Supporting Material (*solid lines*) and the resulting fitting parameters are summarized in Table S1. To see this figure in color, go online.

(i.e., all other compositions) follows somewhat different titration mechanisms. Therefore, it is likely that pHLIP interaction with a pure PC bilayer constitutes a unique case, not representative of its interactions with biological membranes containing multiple lipid species.

The presence of increasing amounts of anionic lipids, such as phosphatidic acid, POPS, POPG, and cardiolipin caused a systematic shift in pK_a and produced higher cooperativity of pH-dependent insertion (i.e., higher n). This pattern is well illustrated in Fig. 2 *B*, which contains titration data for 10, 25, and 75% POPG in a POPC matrix. Increase in anionic lipid content results in an apparent pK_a shift from 5.7, to 6.0, to 6.3 (Table S1). Because a similar pattern is observed for all types of anionic lipids, we conclude that the protonation of key titratable residues in pHLIP, which are responsible for the insertion transition, is modulated by some common property, most likely the electrostatic potential on the membrane interface. High cooperativity of protonation, which manifests itself in the steepness of the insertion transition, has important implications for targeting membranes (or domains) with different compositions. For example, at pH 6, one can expect that insertion of pHLIP will change from virtually nonexistent, to significant, and to complete, for membranes with 10, 25, and 75% of anionic lipids, respectively.

The concept of "local pH" versus "bulk pH" is often invoked in the literature for the explanation of the protonation effects near charged interfaces, like those in Fig. 2 *B*. We consider these explanations to be invalid from a thermodynamic perspective. The reason why protons are concentrated at the PG-containing membrane interface is that they are electrostatically bound to the lipid headgroups. That is, the standard chemical potential of the protons is lower at the charged membrane interface. But the chemical potential of the proton is the same in the bulk solution and at the interface (as required by equilibrium). Therefore, it is equally difficult (or easy) to remove a proton from the interface or from bulk water to attach it to the protein. In other words, the proton concentration (relative activity) is higher at the interface, but this is exactly balanced by tighter association with that same interface. Instead, we suggest that the pK_a values of titratable residues in pHLIP are shifted to higher values by the increasing surface potential. Notably, while the insertion transition is between States I (solution state) and III (inserted state), its properties are modulated by the properties of the interface.

The free energy of protonation ΔG, derived from the pK_a of pHLIP insertion (Eqs. S1 and S2 in the Supporting Material), is plotted against corresponding values of electrostatic surface potential Ψ_0 into POPG-containing membranes (Eq. S3 in the Supporting Material) in Fig. 3 (see also the Supporting Methods in the Supporting Material). The solid line corresponds to a linear approximation based on a Gouy-Chapman electrostatic model that was fixed at −0.023 for

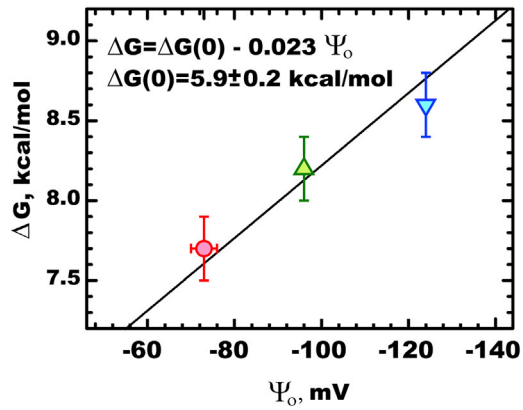

FIGURE 3 Dependence of the free energy of protonation for pHLIP on the electrostatic surface potential of the POPG-containing bilayer (*symbols* correspond to the data in Fig. 2 *B*). See text and the Supporting Material for details. To see this figure in color, go online.

this analysis (see Eqs. S4 and S5 in the Supporting Material). The only free fitting parameter corresponds to a free energy at zero potential, which is found to be 5.9 ± 0.2 kcal/mol. This simplified model appears to accurately represent the data for POPG-containing vesicles.

While the rising dependence of ΔG versus Ψ_0 is observed for every anionic lipid, their slopes are smaller than the one predicted by Gouy-Chapman theory (Table S1). One of the reasons for this is related to the possibility of the lipids themselves to be titrated in the probed region of pH. Such titrations are not expected for PG resulting in a uniform charge across a wide range of pH, and subsequently, pH-independent electrostatic potential. Interestingly, insertion of pHLIP into any of the anionic membranes has higher cooperativity (i.e., larger n) than into neutral membranes (Table S1). The simplest explanation would be that insertion into a bilayer with a negatively charged interface requires protonation of more titratable residues of pHLIP than the insertion in the absence of the electrostatic repulsion.

The interface-directed insertion hypothesis for non-translocon-assembled membrane proteins assigns a special role to the interfacial region of the lipid bilayer as a place where secondary structure is formed, protonation of titratable groups can be changed, and a complex interplay of electrostatic and hydrophobic interactions occurs (9–11). The interface is of a particular importance for the pH-triggered mechanism of membrane protein insertion, which is relevant to cellular entry of bacterial toxins via endosomal pathways and to membrane-modulated interactions of Bcl-2 proteins involved in apoptotic regulation. For example, the kinetics of bilayer insertion of the translocation domain of diphtheria toxin is strongly accelerated by anionic lipids (12). Changes in lipid composition are also important for protonation of titratable residues involved in triggering membrane insertion of the apoptotic inhibitor Bcl-xL (13).

Thus, understanding the nature of lipid modulation of the insertion of pHLIP is relevant to understanding general mechanisms of lipid regulation of signaling and conformational switching on membrane interfaces.

SUPPORTING MATERIAL

Supporting Materials and Methods, Supporting Results, and one table are available at http://www.biophysj.org/biophysj/supplemental/S0006-3495(15)00061-2.

ACKNOWLEDGMENTS

This research was supported by National Institutes of Health grant No. GM-069783.

REFERENCES

1. Andreev, O. A., D. M. Engelman, and Y. K. Reshetnyak. 2014. Targeting diseased tissues by pHLIP insertion at low cell surface pH. *Front. Physiol.* 5:97.
2. Weerakkody, D., A. Moshnikova, …, Y. K. Reshetnyak. 2013. Family of pH (low) insertion peptides for tumor targeting. *Proc. Natl. Acad. Sci. USA.* 110:5834–5839.
3. Andreev, O. A., D. M. Engelman, and Y. K. Reshetnyak. 2010. pH-sensitive membrane peptides (pHLIPs) as a novel class of delivery agents. *Mol. Membr. Biol.* 27:341–352.
4. Wijesinghe, D., M. C. Arachchige, …, O. A. Andreev. 2013. pH-dependent transfer of nano-pores into membrane of cancer cells to induce apoptosis. *Sci. Rep.* 3:3560.
5. Wimley, W. C., and S. H. White. 1996. Experimentally determined hydrophobicity scale for proteins at membrane interfaces. *Nat. Struct. Biol.* 3:842–848.
6. Reshetnyak, Y. K., M. Segala, …, D. M. Engelman. 2007. A monomeric membrane peptide that lives in three worlds: in solution, attached to, and inserted across lipid bilayers. *Biophys. J.* 93:2363–2372.
7. Musial-Siwek, M., A. Karabadzhak, …, D. M. Engelman. 2010. Tuning the insertion properties of pHLIP. *Biochim. Biophys. Acta.* 1798:1041–1046.
8. Fendos, J., F. N. Barrera, and D. M. Engelman. 2013. Aspartate embedding depth affects pHLIP's insertion pK_a. *Biochemistry.* 52:4595–4604.
9. Ladokhin, A. S., and S. H. White. 1999. Folding of amphipathic α-helices on membranes: energetics of helix formation by melittin. *J. Mol. Biol.* 285:1363–1369.
10. Ladokhin, A. S., and S. H. White. 2001. Protein chemistry at membrane interfaces: non-additivity of electrostatic and hydrophobic interactions. *J. Mol. Biol.* 309:543–552.
11. Almeida, P. F., A. S. Ladokhin, and S. H. White. 2012. Hydrogen-bond energetics drive helix formation in membrane interfaces. *Biochim. Biophys. Acta.* 1818:178–182.
12. Kyrychenko, A., Y. O. Posokhov, …, A. S. Ladokhin. 2009. Kinetic intermediate reveals staggered pH-dependent transitions along the membrane insertion pathway of the diphtheria toxin T-domain. *Biochemistry.* 48:7584–7594.
13. Vargas-Uribe, M., M. V. Rodnin, and A. S. Ladokhin. 2013. Comparison of membrane insertion pathways of the apoptotic regulator Bcl-xL and the diphtheria toxin translocation domain. *Biochemistry.* 52:7901–7909.

SUPPORTING INFORMATION

for

Lipid Headgroups Modulate Membrane Insertion of pHLIP peptide

Alexander Kyrychenko,[†] Victor Vasquez-Montes,[†] Martin B. Ulmschneider,[‡]
and
Alexey S. Ladokhin[†]

[†]Department of Biochemistry and Molecular Biology, The University of Kansas Medical Center, Kansas City, KS 66160-7421, U.S.A.

[‡]Department of Materials Science and Engineering, Johns Hopkins University, Baltimore, MD 21218-2608, U.S.A.

MATERIALS AND METHODS

Lipids.

All of the following lipids were purchased from Avanti Polar Lipids (Alabaster, AL): 1-palmitoyl-2-oleoyl-sn-glycero-3-phospholcholine (POPC), 1-palmitoyl-2-oleoyl-sn-glycero-3-phosphoglycerol (POPG), 1-palmitoyl-2-oleoyl-sn-glycero-3-phospho ethanolamine (POPE), 1-palmitoyl-2-oleoyl-sn-glycero-3-phosphoserine (POPS), 1-palmitoyl-2-hydroxy-sn-glycero-3-phosphocholine (lyso-PC), phosphatidic acid (PA), cardiolipin (CL), cholesterol (Chol).

Sample preparation.

Large Unilamellar Vesicles (LUV) were prepared by extrusion as described in (1, 2). Briefly, appropriate volumes of lipid stocks in chloroform were properly mixed and dried under a stream of nitrogen before drying overnight under high vacuum. Dried lipid films were re-suspended and vortexed in 10 mM sodium phosphate buffer (pH 8) to a final concentration of 20 mM of lipid. LUV were prepared by repeated extrusion through a Mini-Extruder from Avanti Polar Lipids (Alabaster, AL) using Nuclepore polycarbonate membranes with 0.1 μm pore size. pHLIP peptide was solubilized in 10 mM phosphate buffer pH 8 to create a stock solution not exceeding 8 μM peptide concentration. For the measurements, the peptide was diluted to 1-2 μM and subsequently mixed with appropriate volume of LUV stock to achieve 1 mM lipid concentration. Membrane insertion was initiated by manual injection of the appropriate aliquots of the 2.5 M acetic buffer, pH 3.2. Samples were incubated for 20 minutes prior to taking measurements.

CD and fluorescence measurements.

CD measurements were performed using an upgraded Jasco-720 spectropolarimeter (Japan Spectroscopic Company, Tokyo). Normally, 20-40 scans were recorded using a 1-mm optical path cuvette. All CD spectra were corrected for background. Fluorescence was measured using an SPEX Fluorolog FL3-22 steady-state fluorescence spectrometer (Jobin Yvon, Edison, NJ) equipped with double-grating excitation and emission monochromators. The measurements were made in a 2×10mm cuvette oriented perpendicular to the excitation beam and maintained at 25°C using a Peltier device from Quantum Northwest (Spokane, WA). Excitation wavelength was 282 nm and the slits were 4 nm. The appropriate background spectra were subtracted in all cases. Spectral analysis was carried out using Origin 8.5 (OriginLab, MA).

Data analysis

pH-dependent changes in spectral position of fluorescence maximum, λ, fitted with the following equation:

$$\lambda = \frac{\lambda_N + \lambda_L \cdot 10^{n \cdot (pK_a - pH)}}{1 + 10^{n \cdot (pK_a - pH)}} \qquad \text{(Eq. S1)}$$

where λ_N and λ_L are the limiting values of the fluorescence maximum at neutral and low pH, respectively; pK_a is an apparent constant and n is a cooperativity coefficient.

Changes in free energy were calculated using a rearrangement of the classical Gibbs free energy formula:

$$\Delta G = 2.3RT(pK_a) \qquad \text{(Eq. S2)}$$

where R is the gas constant and T is the absolute temperature.

Membrane electric potential at bilayer interface, Ψ_o, was calculated using the Gouy-Chapman model(3):

$$\frac{\sigma(8N\varepsilon_o\varepsilon_r\kappa_B T)^{-1/2}}{\sqrt{C}} = \sinh\left(\frac{ze\Psi_o}{2\kappa_B T}\right) \qquad \text{(Eq. S3)}$$

$$\frac{\sigma}{\sqrt{8N\varepsilon_o\varepsilon_r\kappa_B TC}} = \sinh\left(-19.48\Psi_o\right)$$

$$\frac{\sigma}{\sqrt{8N\varepsilon_o\varepsilon_r\kappa_B TC}} = \frac{e^{-19.48\ V^{-1}(\Psi_o)} - e^{19.48\ V^{-1}(\Psi_o)}}{2}$$

where σ is the surface charge density of charges of the membrane created by anionic lipids, N is the Avogadro constant, ε_o is the permittivity in vacuum, ε_r is the dielectric constant of water (78.3), k_B is the Boltzman constant, C is the ion concentration of valence z, and e is the elementary charge. Solving this equation for the buffer system used (10 mM sodium phosphate) and assuming constant lipid charge throughout the titration, results in a surface electrostatic

potential of -73 mV, -96 mV and -124 mV for 10, 25 or 75% POPG in POPC matrix, respectively (Fig. 3).

The effect of the electric potential on protonation at the interface was described as suggested by Fernandez and Fromherz (4):

$$pK_a = pK^{\text{int}} - \frac{F_o \Psi_o}{2.3RT} \qquad \text{(Eq. S4)}$$

where pK_a is the apparent pK (experimental) and pK^{int} is the intrinsic pK, F_o is the Faraday constant, T is the absolute temperature, R is the gas constant, and Ψ_o is the membrane surface electrostatic potential calculated from Eq. S3.

Combining Eqs. S2 and S4 results in the following linear dependence of free energy vs surface potential, which was used to fit the data in Fig. 3:

$$\Delta G = 1.363 pK^{\text{int}} - 0.023 \tfrac{kcal}{mol \cdot mV} \Psi_o = \Delta G(0) - 0.023 \tfrac{kcal}{mol \cdot mV} \Psi_o \qquad \text{(Eq. S5)}$$

where $\Delta G(0)$ is the only free fitting parameter.

SUPPLEMENTAL RESULTS

Numerous studies demonstrate that pHLIP can interact with phosphatidylcholine bilayers in which it has been shown to be either associated interfacially at neutral pH (state II, according to designation of Engelman and co-workers) or inserted across the bilayer at low pH (state III) (5-7). These states are characterized by blue shifted tryptophan fluorescence and increased helical structure, which distinguishes them from unfolded state formed by pHLIP in solution at neutral pH (state I). Our measurements with POPC LUV accurately reproduce these features (Fig. 1). However, the presence of the state II was not observed in any of the LUV compositions tested, as indicated by the lack of changes in fluorescence and ellipticity between states I and II (Fig. 1, Table ST1). LUV containing LysoPC are the only other vesicles (in addition to pure POPC) that induce some spectral shift in pHLIP at neutral pH (Table ST1), however, it can't be excluded that in this case the peptide interacts with the lyso-lipid outside of the bilayer.

The obtained pK_a values were converted to free energy using Eq. S2. In the case of POPG vesicles the ΔG was plotted against the surface electrostatic potential (Ψ_o); which was obtained

using the Gouy-Chapman model (Eq. S3). These calculations were performed under the assumption that the protonation state of the lipids was stable. This assumption, however, does not hold for anionic lipids other than POPG (8-10), for which this analysis was not performed.

Table S1. Summary of pH-dependent interactions of pHLIP with LUV of various lipid compositions. Presence of pHLIP state II and III were determined by comparing shifts in tryptophan fluorescence maxima in the presence of vesicles at neutral (λ_N) and acidic pH (λ_L) with respect to the fluorescence maxima in state I (358nm), pHLIP in solution at neutral pH (Fig. 1). The four parameters characterizing pH-dependent insertion of pHLIP, namely λ_N, λ_N, pK_a and n were obtained by nonlinear least-square fit with Eq. S1 of pH titration of intrinsic fluorescence spectral data (e.g., Fig. 2). ΔG was calculated from the observed pK_a values using Eq. S2.

Lipids mol:mol	*State II*	λ_N *(nm)*	*State III*	λ_L *(nm)*	pK_a *± 0.1*	*n* *±0.3*	$\Delta G \pm 0.2$ *(kcal/mol)*
POPC	+	353	+	343	6.1	1.2	8.3
POPC:POPE 9:1	-	357	+	343	5.7	1.6	7.8
POPC:POPE 1:1	-	357	+	341	6.2	1.3	8.5
POPC:Chol 4:1	-	358	+	343	6.1	1.6	8.3
POPC:lysoPC 4:1	+/-	355	+	343	6.0	1.2	8.2
POPC:POPG 9:1	-	358	+	342	5.7	4.3	7.8
POPC:POPG 3:1	-	358	+	341	6.0	3.0	8.2
POPC:POPG 1:3	-	358	+	341	6.3	2.5	8.5
POPC:CL 6:1	-	358	+	341	6.1	2.6	8.3
POPC:CL 2:3	-	358	+	341	6.2	2.0	8.5
POPC:POPS 9:1	-	358	+	342	6.0	4.4	8.2
POPC:POPS 3:1	-	358	+	342	6.1	2.7	8.3
POPC:PA 9:1	-	358	+	341	5.8	2.5	7.9
POPC:PA 1:3	-	358	+	341	5.9	3.0	8.0

References

1. **Hope, M. J., M. B. Bally, L. D. Mayer, A. S. Janoff, and P. R. Cullis. 1986. Generation of multilamellar and unilamellar phospholipid vesicles. Chem.Phys.Lipids 40:89-107.**
2. **Mayer, L. D., M. J. Hope, and P. R. Cullis. 1986. Vesicles of variable sizes produced by a rapid extrusion procedure. Biochim.Biophys.Acta 858:161-168.**
3. **McLaughlin, S. 1989. The electrostatic properties of membranes. Annual review of biophysics and biophysical chemistry 18:113-136.**
4. **Fernandez, M. S., and P. Fromherz. 1977. Lipoid pH indicators as probes of electrical potential and polarity in micelles. J.Phys.Chem. 81:1755-1761.**
5. **Hunt, J. F., P. Rath, K. J. Rothschild, and D. M. Engelman. 1997. Spontaneous, pH-dependent membrane insertion of a transbilayer α-helix. Biochemistry 36:15177-15192.**
6. **Barrera, F. N., J. Fendos, and D. M. Engelman. 2012. Membrane physical properties influence transmembrane helix formation. Proc Natl Acad Sci U S A 109:14422-14427.**
7. **Reshetnyak, Y. K., M. Segala, O. A. Andreev, and D. M. Engelman. 2007. A monomeric membrane peptide that lives in three worlds: in solution, attached to, and inserted across lipid bilayers. Biophys J 93:2363-2372.**
8. **Kooijman, E. E., and K. N. Burger. 2009. Biophysics and function of phosphatidic acid: a molecular perspective. Biochimica et biophysica acta 1791:881-888.**
9. **Olofsson, G., and E. Sparr. 2013. Ionization constants pKa of cardiolipin. PloS one 8:e73040.**
10. **Tsui, F. C., D. M. Ojcius, and W. L. Hubbell. 1986. The intrinsic pK_a values for phosphatidylserine and phosphatidylethanolamine in phosphatidylcholine host bilayers. Biophys.J. 49:459-468.**